Arch. Metall. Mater. **64** (2019), 3, 1151-1162

DOI: 10.24425/amm.2019.129508

J. MARCISZ*#, J. JANISZEWSKI**

MECHANICAL BEHAVIOUR OF NANOSTRUCTURED BAINITIC STEEL UNDER HIGH STRAIN RATE SHEAR AND COMPRESSION LOADING

The article presents the results of investigation of ultra-strength nanostructured bainitic steel Fe-0.6%C-1.9%Mn-1.8%Si-1.3%Cr-0.7%Mo (in wt. %) subjected to shear and uniaxial compression under high strain rate loading. Steel of microstructure consisted of carbide-free bainite and carbon enriched retained austenite presents a perfect balance of mechanical properties especially strength to toughness ratio. Two retained austenite morphologies exist which controlled ductility of the steel: film between bainite laths and separated blocks. It is well established that the strain induced transformation of carbon enriched retained austenite to martensite takes place during deformation. Shear localisation has been found to be an important and often dominant deformation and fracture mode in high-strength steels at high strain rate. Deformation tests were carried out using Gleeble simulator and Split Hopkinson Pressure Bar. Shear and compression strength were determined and toughness and crack resistance were assessed. Susceptibility of nanostructured bainitic steel to the formation of adiabatic shear bands (ASBs) and conditions of the bands formation were analysed. The results suggest that the main mechanism of hardening and failure at the dynamic shearing is local retained austenite transformation to high-carbon martensite which preceded ASBs formation. In the area of strain localization retained austenite transformed to fresh martensite and then steel capability to deformation and strengthening decreases.

Keywords: nanostructured bainitic steel, high strain rate material properties, adiabatic shear bands, shear energy

1. Introduction

Steel with microstructure consisting of nanometre size, carbide-free bainite laths and retained austenite offers an unique combination of static strength and ductility. Ductility behaviour of the steel under dynamic shear and compression loading is interesting due to shear localisation which has been found to be an important deformation and fracture mode in metals at high strain rates.

Nanostructured bainitic steels have been the subject of investigation of many research and development centres for over a dozen years [1-7]. The material belongs to ultra-strength steels with ultimate tensile strength (UTS) exceeding 2 GPa and total elongation in tensile static test over 12% [5,6]. Microstructure of the steel consists of carbide-free lower bainite laths which form as a result of isothermal heat treatment directly after austenitisation and controlled cooling. The fine plates of carbide-free bainite are separated by untransformed carbon enriched retained austenite. Moreover blocks of retained austenite separating the sheaves of packets of bainite. Then, there is the possibility of improving simultaneously the strength and toughness because of the nanolaths of the bainite and by a transformation induced plasticity effect (TRIP) that increases the strain-hardening rate and guarantees good ductility [8-10]. The mechanical stability of the austenite is controlled by its chemical composition and its morphology (blocks or thin films) [9]. Work on the factors controlling the ductility of the nanobainite, especially relationship between austenite stability and static tensile ductility suggested the existence of critical value beyond which brittle behaviour cannot be avoided [11,12].

Nanostructured bainitic steels are used, among others, as armour components due to the high level of strength and crack resistance during multi-hit firing tests [13-15]. Analysis of mechanisms of interaction of armour plate with the core of a different type of projectiles indicate that shear strength, energy of shearing and plastic deformation capacity in shear test are crucial parameters responsible for resistance to perforation [13-16]. Moreover, during deformation with high strain rate and additionally on impact, adiabatic shear bands (ASBs) can form in the vicinity of the hit points [17-20]. One problem that has delayed understanding of the shear banding phenomenon is the difficulty of comparing results obtained from the different types of laboratory tests that have been developed, because shear bands will usually nucleate from geometrical defects in preference to microstructural defects [19]. Conditions of the formation of this type of microstructure heterogeneity are crucial for crack sensitivity of the material. It has been known that ASBs form most readily in alloys of low thermal conductivity such as steels

* ŁUKASIEWICZ RESEARCH NETWORK-INSTITUTE FOR FERROUS METALLURGY, 12-14 KAROLA MIARKI STR., 44-100, GLIWICE, POLAND
** MILITARY ACADEMY OF TECHNOLOGY, 2 GEN. SYLWESTRA KALISKIEGO STR., 00-908 WARSZAWA, POLAND
# Corresponding author: jaroslaw.marcisz@imz.pl

[20]. Cracks can often propagate within shear bands more easily than through the matrix [15,16].

Dynamic properties of nanostructured bainitic steels at a strain rate of up to several thousand s^{-1} have been determined with the use of the Split Hopkinson Bar technique (SHB) in tensile and compression tests [14,21]. The dynamic yield strength of about 2600 MPa and strain of about 0.2 were achieved for nanostructured bainite at strain rate 3290 s^{-1} in compression tests [14]. Nanostructured bainitic steel examined by authors [21] characterized by low strength about 1500 MPa determined in static tensile test. The authors [21] reached engineering stress level about 2400 MPa at strain rate 1820 s^{-1} under compression test and suggested that TRIP effect is not occurred and caused of lower amount of dynamic deformation. Changes of mechanical properties and microstructure of nanostructured bainitic steel (Fe-0.79%C-2.16%Si-2.02%Mn-1.36%Cr) under dynamic compression using Hopkinson bar were discussed [22,23]. Deformation twins of nanometre size in the blocky and lathy retained austenite after compression were found. They found also fresh martensite (α') as a result of TRIP effect occurring. Twinning is a dominant mechanism of deformation which occurs firstly in blocky austenite and next in the retained austenite in form of laths between bainite laths. Three different responses in blocky austenite were found, as follows: mechanical twins with a kinked morphology, one variant of primary mechanical twins, and two variants of primary mechanical twins with α' martensite. For film austenite, single variant of twinning can be dominant. All those deformation modes involved twinning, implying that nanostructured bainite can trigger the twinning-induced plasticity effect (TWIP) when it is deformed at a strain rate of 10^3 s^{-1}. In contrast, retained austenite in nanostructured bainite is well-known to transform into fresh martensite during quasi-static tensile tests [8,9,12].

Adiabatic shear bands of width 10 mm were found in the dynamically compressed steel grade 4340 using Hopkinson method [24]. The final fracture path coincides with adiabatic shear bands. The structure of the bands generated by ballistic testing were examined in order to reveal the governing mechanisms [25]. The authors attempt to distinguish in particular whether local reaustenitisation occurs, or if the microstructural change are a reflection simply of intense deformation. The bands consist of deformed layers in which the original structure becomes mechanically mixed, and resembles a warm-worked microstructure that is still in an unrecrystallised state. Adiabatic shear bands are unlikely to represent phase transformation from retained austenite that forms during adiabatic heating and transforms subsequently into martensite [25].

This article presents the results of investigation of properties of nanostructured bainitic steel determined under dynamic shear and compression tests. Maximum stress and energy of dynamic shearing were determined and microstructure examination and hardness measurement, especially within areas of strain localisation, were carried out. Role of retained austenite in the dynamic deformation process realised by shear mode was discussed. The effect of adiabatic shear bands on the properties of the nanobainite steel was analysed.

2. Experimental procedures

High strain rate shear and compression tests were carried out with the use of a Gleeble 3800 simulator. Shear experiments with punch velocity in the range of 0.3÷800 mm/s and uniaxial compression at strain rate in the range of 1÷100 s^{-1} were conducted. The experimental setup scheme of the punch and die used in shearing tests and plane of microstructure examination are presented in Fig. 1a. Square 25×25 mm specimens with a nominal thickness of 3.0 mm were used in the shearing tests. The diameter of the punch was 5.90 mm and the diameter of the die hole was 6.0 mm for Gleeble tests (Fig. 1b). Cylindrical specimens with a diameter of 6.0 mm and a height of 7.0 mm were used in uniaxial compression experiments in Gleeble simulator. In a standard uniaxial compression test, the specimen is fixed between two anvils before the beginning of deformation (Fig. 2a), while no direct impact of the anvil on the specimen occurs. A deformation mode was developed to produce a direct impact effect on surface of the compressed specimen. A spacing between the sample and the anvil was applied in a modified experimental setup (Fig. 2b). Shear tests were also carried out using Split Hopkinson Bar technique (SHB) at punch velocity from 5.0 to 10.2 m/s with the use of the punch and die setup similar to one applied in Gleeble experiments (Fig. 3). Specimens of diameter 25 mm with a thickness of 2.0 mm were used in the shearing tests in SHB using punch diameter of 3.9 mm and die hole diameter of 4.0 mm.

As a result of shearing experiments, shear strength and energy of shearing at the punch velocity in the wide range of 0.3÷10200 mm/s were determined. Moreover, the toughness of the steel defined as a punch displacement until shear failure was assessed. Volume fraction of material subjected to shearing depended on difference in punch and die diameters and on the specimen thickness. Based on the stress-strain compression curves, maximum stress and strain were determined at the strain rates: 1, 10 and 100 s^{-1} under direct and indirect loading.

Microstructure examination, especially in the area of strain localisation, were carried out using a light microscope and scanning electron microscope. Metallographic samples were etched using nital agent to reveal the phases. Hardness distribution in the vicinity of shear bands was determined in micro-Vickers tests for 25 gf loads. Based on the hardness results maps of hardness distribution were worked out. The determination of volume fraction of retained austenite of deformed specimens in the shear zones was achieved by means of X-ray microdiffraction method with the use of monocapillary and Averbach-Cohen method. The diameter of examined area in the deformed region of specimen was about 100 μm. Surface temperature measurements during cold compression tests without additional water or air cooling in Gleeble using a thermocouple were carried out. Temperature within the range of 210÷320°C was detected as a result of dynamic direct compression. The temperature measurement results describe conditions of the deformation experiments. The effect of temperature on the deformation process, particularly on the adiabatic shear bands formation was not analysed.

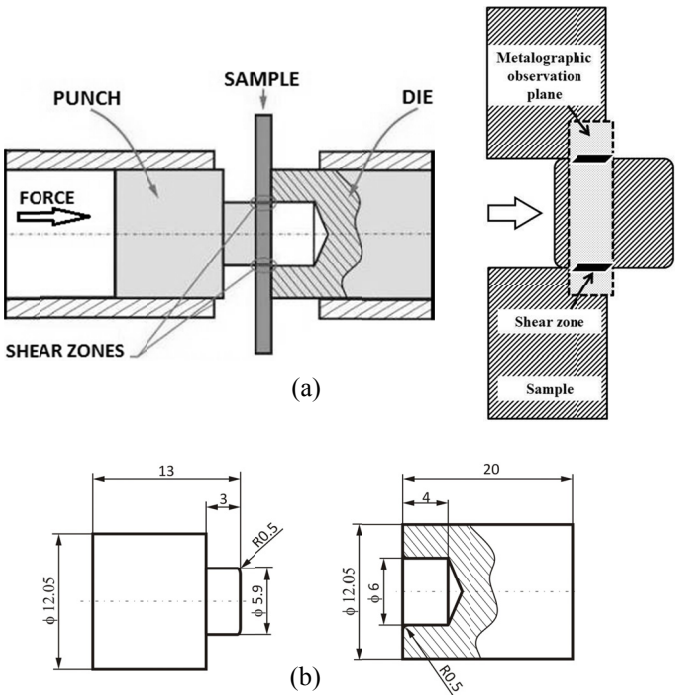

Fig. 1. Experimental setup applied in shearing tests using Gleeble simulator (a), diameters of punch and die used in experiments (b)

3. Material

Sheets with a thickness of 3 to 12 mm made of bainitic steel were used as the study material. 24 tonne industrial heat of nanostructured bainite steel was melted in an electric arc furnace (EAF). Liquid steel was subjected to vacuum arc degassing (VAD) to obtain required cleanliness. The heat was cast into six ingots of about 4 tonnes each, using a bottom casting method. The ingots were homogenised at 1200°C during 24 hours and directly hot forged into flat bars. From the flat transfer bars, plates with thickness form 3 to 12 mm were hot rolled. The final heat treatment consisted of austenitising at 950°C during 30 minutes, controlled air cooling from austenitising temperature with the rate higher than 1°C/s to a temperature of the isothermal heat treatment and isothermal transformation into lower bainite at a temperature of 210°C for 120 hours. After isothermal holding, cooling in the still air to the ambient temperature was applied.

Chemical composition of the examined material is presented in Table 1. As a result of applying temperature and time of isothermal holding: 210°C and 120 hours (B-210), mechanical properties and morphology of microstructure were produced characterize of nanostructured bainite. Table 2 shows the average values of selected properties of the investigated nanostructured bainitic steel: hardness, mechanical properties determined in static tensile test, as well as impact strength and volume fraction of retained austenite. Engineering stress-strain curve of the examined nanobainitic steel was presented in Fig. 4. Tensile deformation of nanostructured bainite is characterized by plain stress-strain curves with continuous strengthening, high tensile strength to yield strength ratio and relatively large uniform elongation. The steel microstructure observed using a scanning

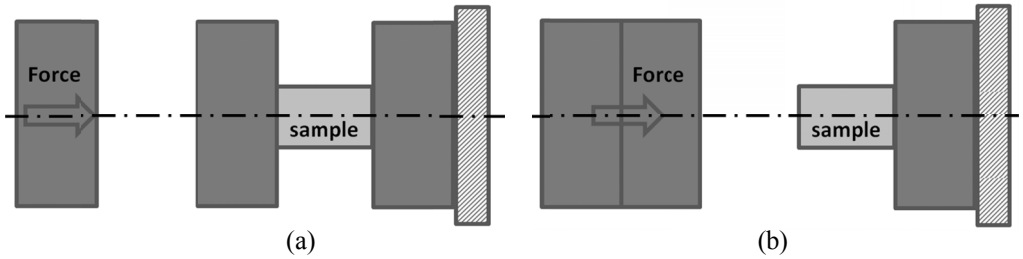

Fig. 2. Experimental setup applied in uniaxial compression using Gleeble simulator. (a) indirect loading, (b) direct loading

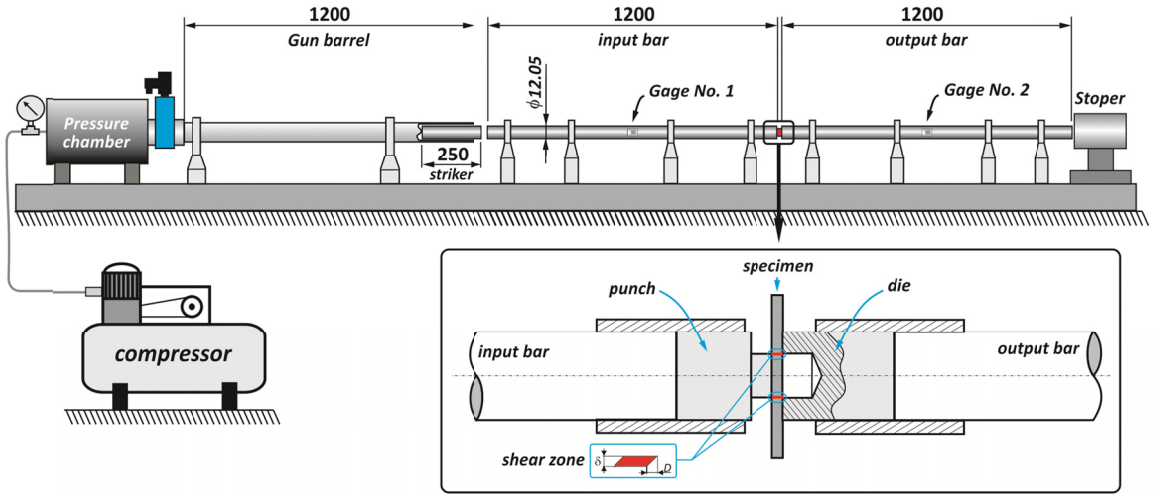

Fig. 3. Split Hopkinson Pressure Bar testing system

TABLE 1

Chemical composition of nanostructured bainitic steel and calculated Ms temperature, weight %

C	Mn	Si	P	S	Cr	V	Mo	Ti	Ms*, °C
0.58	1.90	1.82	0.012	0.005	1.32	0.095	0.75	0.010	201

*) Ms = 539-423%C-30,4%Mn-12,1%Cr-7,5(%Si+%Mo)

electron microscope and EBSD analysis results are presented in Fig. 5. Packets of bainite laths and blocks of retained austenite in the form of separated grains were observed in the steel using EBSD technique (Fig. 5b). Volume fraction of retained austenite of 20% were determined using X-Ray technique. Based on the EBSD analysis it was found that volume fraction of blocky retained austenite was about 12%. It means that the volume fraction of retained austenite in form of nanolaths situated between bainite laths was about 8%. Nanolaths of bainite and film of retained austenite between bainite were observed in transmission electron microscope (Fig. 6).

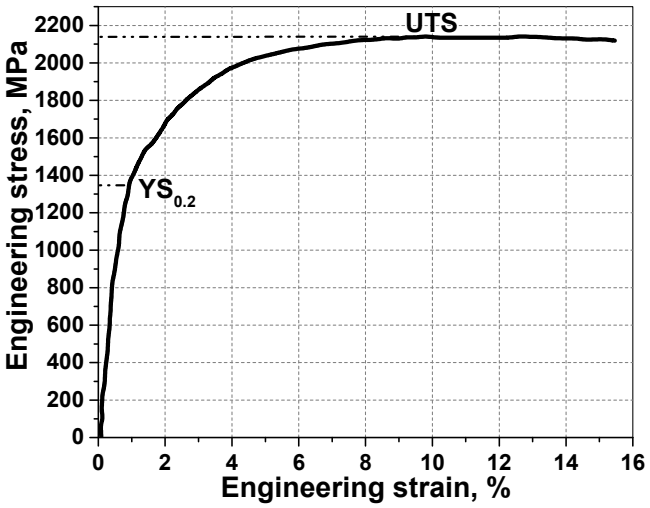

Fig. 4. Engineering stress-strain curve of B-210 nanostructured bainite. Static tensile test

4. Results and discussion

4.1. Shearing tests in Gleeble simulator

The shearing stress vs. punch displacement curves are presented in Fig. 7. The B-210 variant of nanostructured bainitic steel is characterised by the shear strength within the range of 1400÷1550 MPa at the applied punch velocities. It was clearly showed that punch displacement substantially decreased at velocity above 3 mm/s. Nanostructured bainitic steel B-210 is characterised by the highest shear stress at the punch velocity of up to 30 mm/s. The shear stress dropped to about 1400 MPa with punch velocity increased up to 800 mm/s (Fig. 8).

Figs. 9÷11 show the results of macro- and microstructure examination and hardness measurements within the shear zone

TABLE 2

Static mechanical properties, impact toughness and volume fraction of retained austenite

Material's denotation	Yield strength, $YS_{0.2}$, MPa	Ultimate tensile strength, UTS, MPa	Total elongation, E_t, %	Uniform elongation, E_u, %	Hardness, HV	Notch impact toughness (Charpy-V), J		Volume fraction of retained austenite, %
						+20°C	–40°C	
B-210	1350	2140	12.0	10.0	600÷620	23	13	20

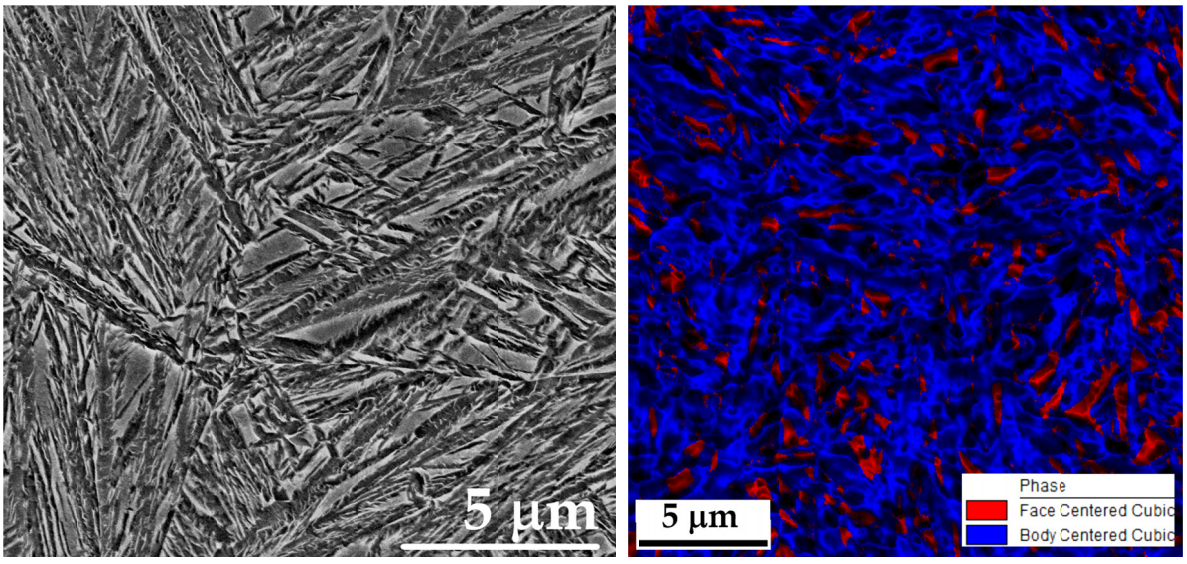

(a) (b)

Fig. 5. Microstructure (a) and EBSD phase map (b) of B-210 nanostructured bainitic steel. Scanning electron microscope, FCC-blocky retained austenite, BCC-packets of bainite laths

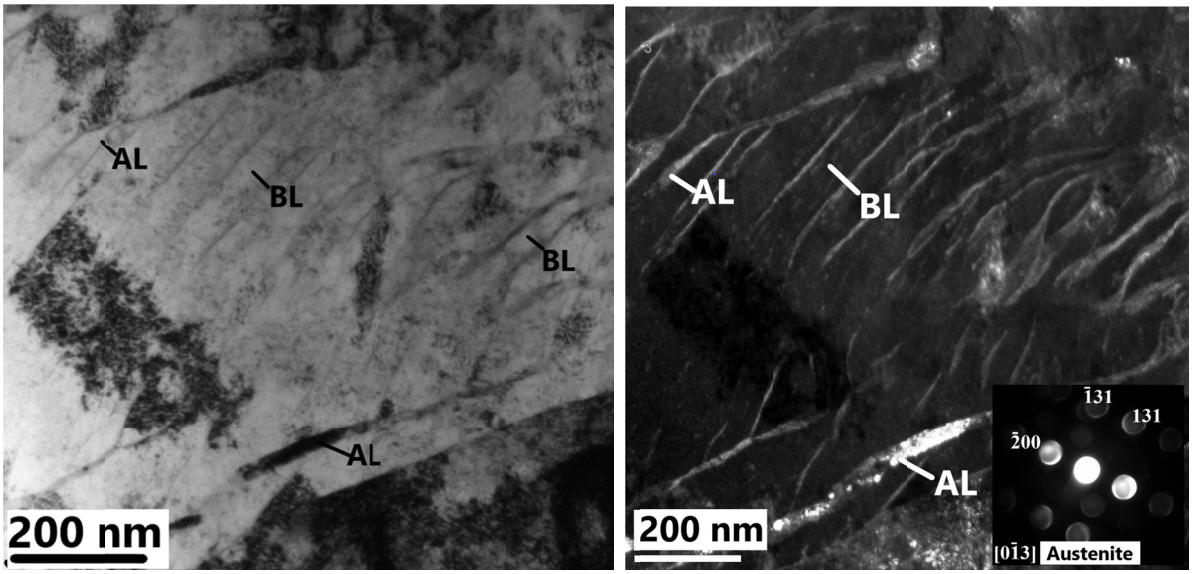

(a) (b)

Fig. 6. Microstructure of B-210 nanostructured bainitic steel. (a) BF transmission electron microscope image, (b) DF image in austenite reflection and diffraction pattern of austenite, AL-nanolaths of retained austenite, BL-nanolaths of bainite

for the B-210 nanostructured bainitic steel. Hardness increasing up to 720 HV was detected within shear zone without ASB (Fig. 9). In the vicinity of the bands, an area with a width ranging from 0.2 to 0.4 mm with hardness exceeding 800 HV was found (Fig. 10). The increase in hardness of the region of strain localization resulted from transformation of retained austenite to fresh martensite. Adiabatic shear bands of hardness within the range of 850÷930 HV visible as non-etched white lines on the steel microstructure background were found at higher punch displacement (Fig. 11).

Microstructure of the band of the examined steel variant B-210 consist of two regions of different morphology (Fig. 11b). In the centre of the band fine-grained microstructure was observed and in the vicinity of the non-deformed matrix the microstructure consist of strongly elongated packets of bainite laths parallel to the band. Microcracks were found inside the bands, which would propagate along the band and occasionally to the steel matrix.

Deformation mode and the strain rate both are influence the mechanical stability of retained austenite. Measurements of volume fraction of retained austenite using microbeam X-ray technique were carried out in the shear zone to confirm the phase transformation to martensite. The diameter of the measured regions, especially around the ASB was shown in Fig. 12. Initial retained austenite content in the examined steel variant B-210 was 20.4%. It was found that volume fraction of retained austenite decreases in the shear zone to 10.3%. It is necessary to highlight that average volume fraction of martensite is about 10%. Martensite is non-uniformly distributed in the measured area around the ASB according to hardness distribution results. The determined volume fraction of about 10% refers to the average content of retained austenite in form of laths and blocks in the area of X-ray examination.

The results suggest that at the dynamic shearing the main mechanism of hardening and failure is local retained austenite transformation to high-carbon martensite which preceded ASBs

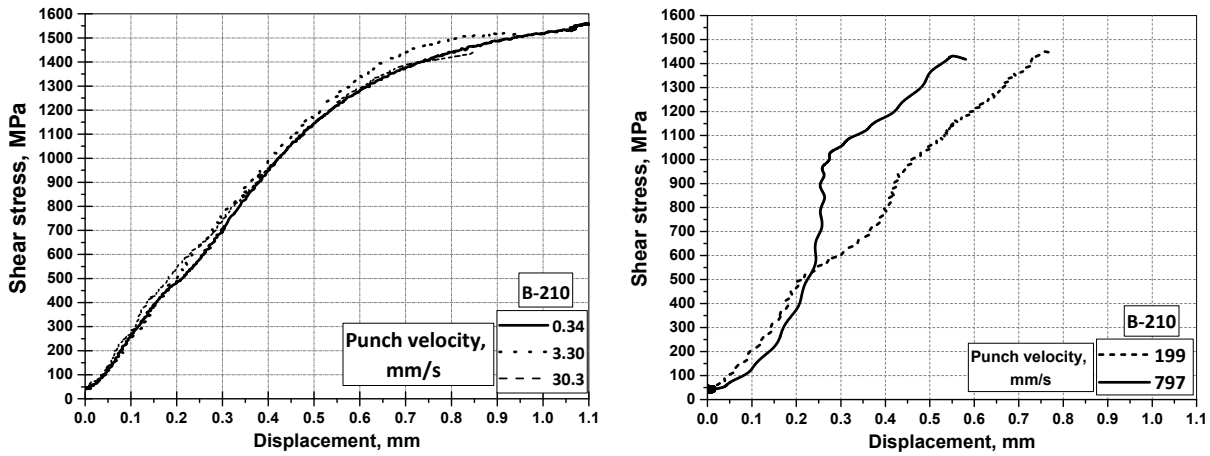

Fig. 7. Shear stress vs. punch displacement. Nanostructured bainitic steel B-210

formation. Mechanical stability of the austenite is the crucial factor which control toughness of the nanostructured bainite [8,9,11,12]. In the area of strain localization retained austenite transformed as a result of deformation to martensite and then steel capability to deformation and strengthening decreases. Formation of the ASBs preceded by local hardness increasing up to about 800 HV consumed energy of dynamic deformation but reduced toughness of the steel.

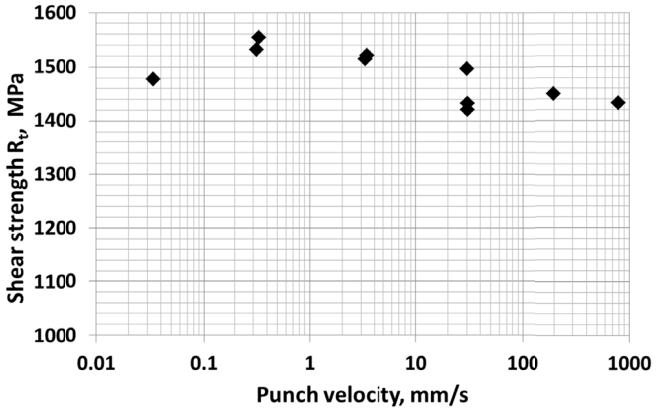

Fig. 8. Shear strength vs. punch velocity in the range up to 800 mm/s. Nanostructured bainitic steel B-210

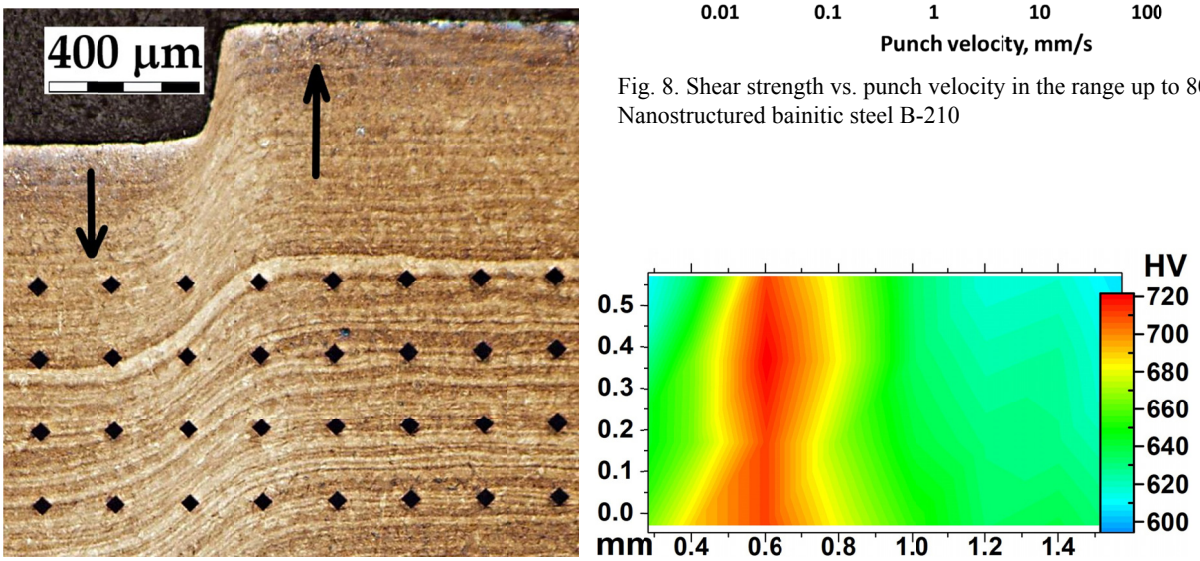

Fig. 9. Macrostructure and hardness distribution within the shear zone without ASB. Nanostructured bainitic steel – variant B-210; punch velocity of 0.3 mm/s; punch displacement of 0.3 mm

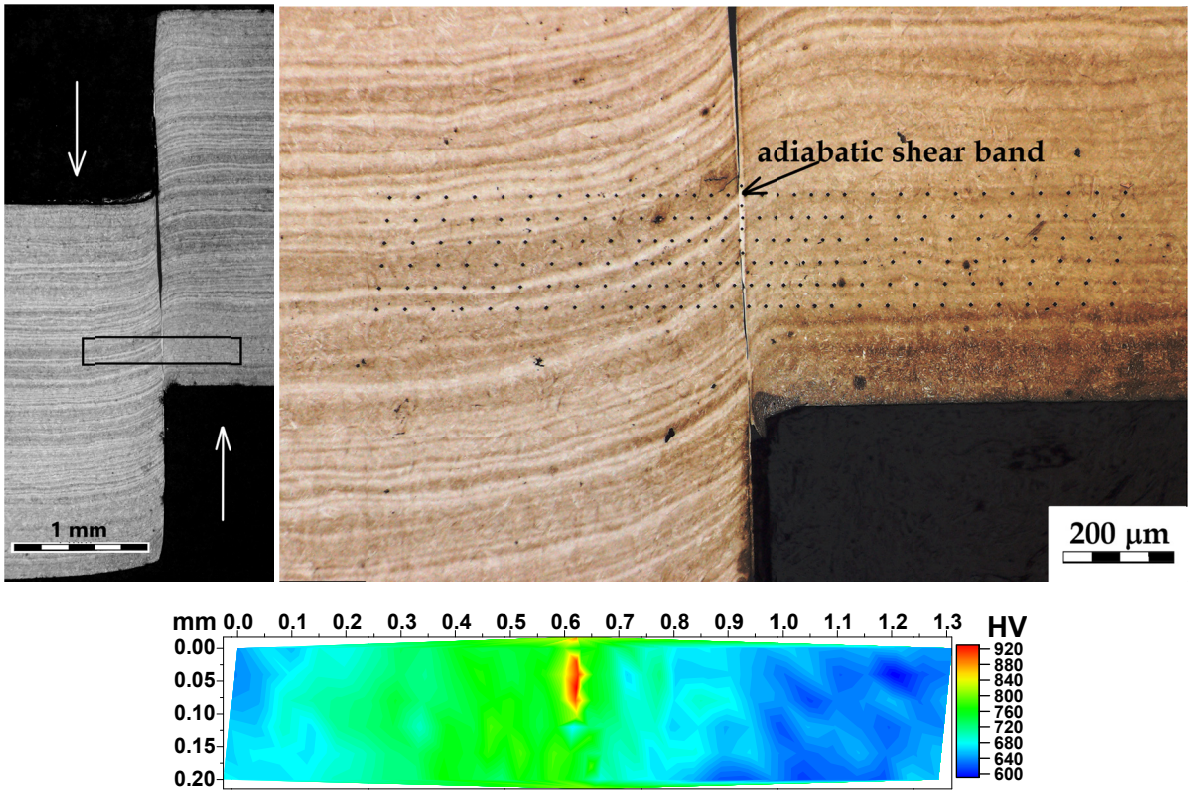

Fig. 10. Macrostructure and hardness distribution within the shear zone with ASB. Nanostructured bainitic steel: variant B-210; punch velocity of 30.4 mm/s; punch displacement of about 0.85 mm

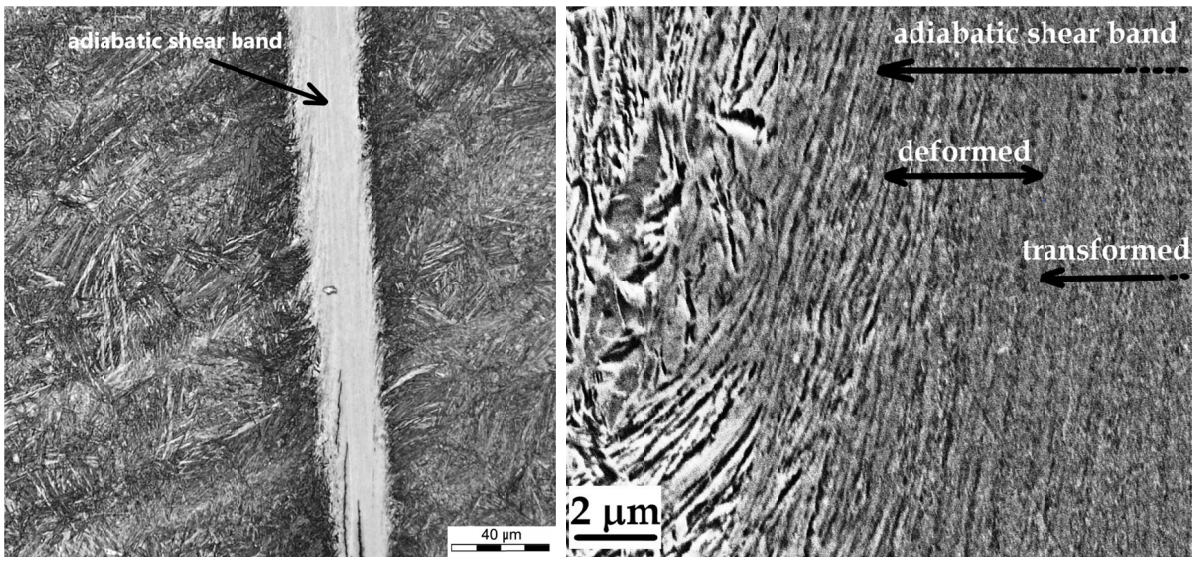

(a) (b)

Fig. 11. Microstructure within the area of adiabatic shear band. Nanostructured bainitic steel: variant B-210 – punch velocity of 797 mm/s; punch displacement of 0.55 mm; (a) light microscope; (b) scanning electron microscope

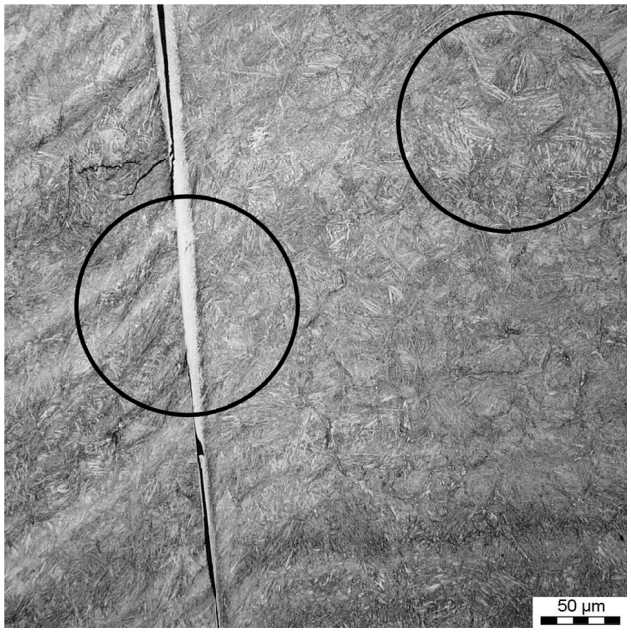

Fig. 12. Areas of retained austenite volume fraction measurements using microbeam X-ray technique. B-210 variant of nanobainite deformed using Gleeble simulator at punch velocity of 30.4 mm/s

4.2. Shear tests with the use of Hopkinson bar

The dynamic shear stress vs. punch displacement curves are presented in Fig. 13. The B-210 variant of nanostructured bainitic steel is characterised by the maximum shear stress of 1460 MPa at the punch velocities of 10.2 m/s. Punch displacement to shear failure of specimens in the range of 0.25÷0.30 mm were found for examined B-210 steel variant. In comparison to high-strength martensitic armour steel (UTS about 2000 MPa) characterised by the dynamic shear strength of 1200 MPa [26], tested steels revealed higher shear stress level.

Figs. 14 and 15 show the results of macro- and microstructure examination and hardness measurements within shear zone for the B-210 nanostructured bainitic steel. Hardness increasing up to 670 HV was detected in deformed shear zone without ASB (Fig. 14a), whereas adiabatic shear bands with hardness up to 1150 HV visible as non-etched white lines on the steel microstructure background were found at higher punch displacement and velocity (Fig. 15b). In the vicinity of the bands, narrow zone with a width of about 0.2 mm with hardness ranging from 700 to 800 HV was observed.

Measurements of volume fraction of retained austenite using microbeam X-ray technique were carried out to confirm the phase transformation to martensite. The diameter of the measured regions around the ASB was shown in Fig. 16. Retained austenite content in the examined steel variant B-210 was 20.4% and volume fraction of blocky austenite was 12%. It was found that volume fraction of retained austenite decreases in the shear

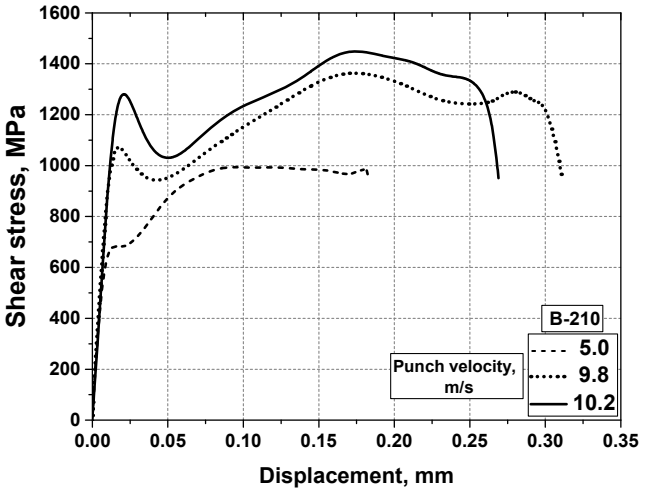

Fig. 13. Dynamic shear stress vs. punch displacement. Nanostructured bainitic steel

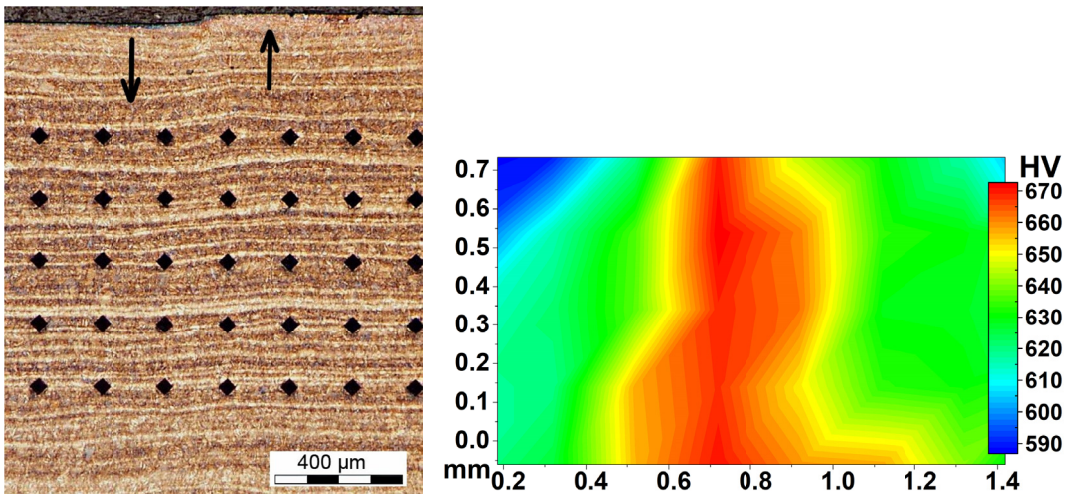

(a) (b)

Fig. 14. Macrostructure (a) and hardness distribution (b) in the vicinity of shear zone. Punch velocity of 5.0 m/s (shear zone without ASB). Nanostructured bainite, variant B-210, SHB shear test

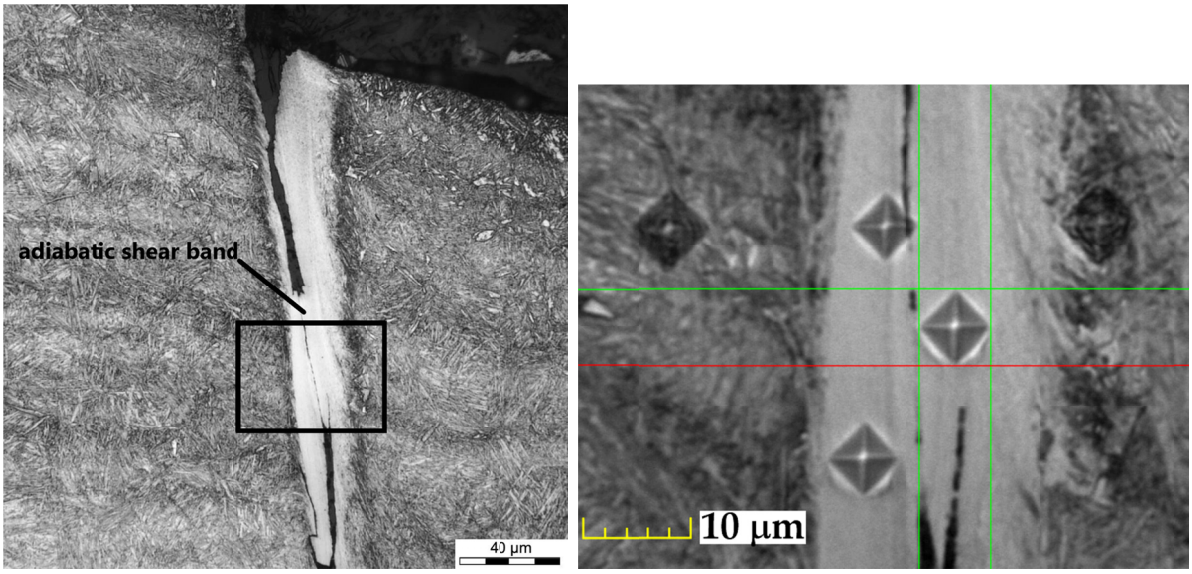

(a) (b)

Fig. 15. Microstructure of adiabatic shear band (a) and hardness impressions in the area of the band (b). Punch velocity of 9.8 m/s. Nanostructured bainite, variant B-210, SHB shear test

zone to 8.6%. It means that average content of martensite in the shear zone is about 12%. Blocky austenite was assumed to be less stable and thus to be deformed first [22]. It is possible that in the shear zone total content of blocky austenite transformed to martensite. The results show that the high-carbon retained blocky austenite plays an important role in energy absorption during the shearing.

4.3. Energy of dynamic shearing

It is important to be able to predict the energy level consumed by shearing with ASBs formation process which describes the energy absorption and dissipation ability of the steel. Based on the force-displacement curves $Fs = f(s)$, the energy of dynamic shearing with ASBs formation (defined as an area under the curve) was determined:

Total energy of shearing (E_t): $E_t = \int_0^{st} F_s ds$

where st – punch displacement to shear failure of specimen.

The shear energy was determined in the range of punch velocity from 0.03 to 10200 mm/s based on the test results obtained from Gleeble and SHB experiments. For shear energy determination, experiments with failure of specimen by reason of adiabatic shear bands formation were selected. In SHB experiments, the strain rate (and the strain value) can be controlled only by the incident bar velocity, and we cannot shear the specimen at all required strain rates. In Gleeble simulator, because of the

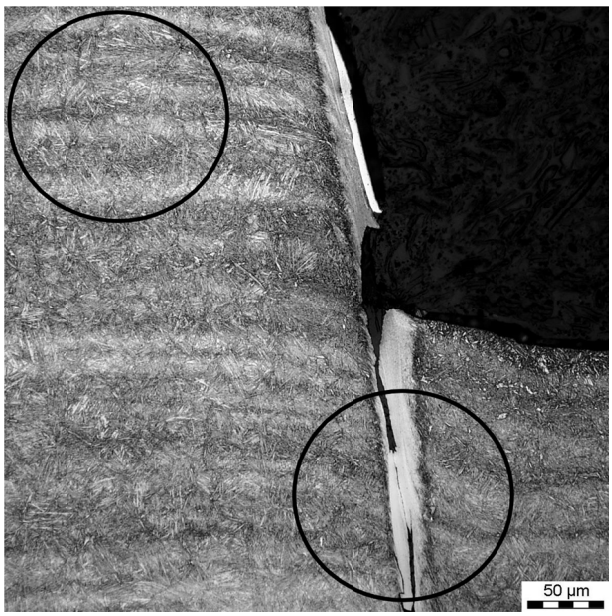

Fig. 16. Areas of retained austenite volume fraction measurements using microbeam X-ray technique. B-210 variant of nanobainite deformed using SHB method at punch velocity of 9.8 m/s

hydraulic system of punching, we can shear specimen at all scheduled strain rates.

The relatively constant shear energy with punch velocity up to 3.0 mm/s was observed. It is evident that increase the punch velocity from 3.0 to 797 mm/s resulted in decrease of total shear energy of nanostructured bainitic steel from 13 to 6×10^9 J/m^3 (Fig. 17). Two factors influence the shear energy of the nanostructured bainite: shear stress and strain defined as punch displacement. The main factor responsible for value of shear energy is ductility which clearly decreased with strain rate increasing.

At the punch velocity of about 10 m/s in Hopkinson bar experiments the shear energy of $7\div8\times10^9$ J/m^3 for B-210 variant was determined (Fig. 18). At the punch velocity of about 5 m/s no failure of specimens occurred and then energy of shearing

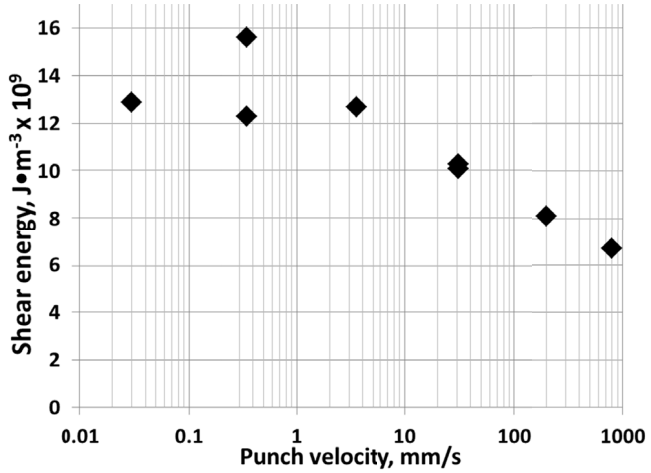

Fig. 17. Normalised (related to volume of shear zone resulted from the difference between diameter of the punch and die) total shear energy vs. punch velocity (Gleeble simulator)

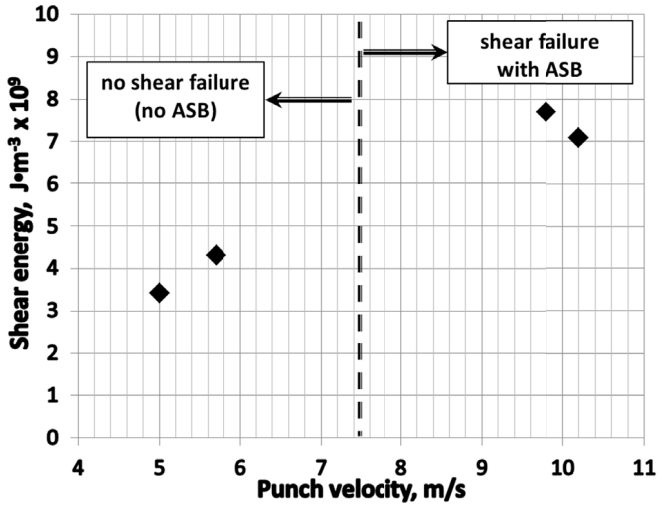

Fig. 18. Shear energy vs. punch velocity, (a) related to volume of shear zone resulted from the difference between diameter of the punch and die; (SHPB experiments)

was not calculated (Fig. 18). It suggests that propensity to transformation of retained austenite to fresh martensite depends on both strain rate and strain value.

4.4. Direct and indirect compression in Gleeble simulator

The influence of loading method (direct and indirect) under Gleeble simulator conditions with strain rates of 1, 10 and 100 s^{-1} on dynamic compression stress and strain of nanostructured bainitic steel (variant B-210) is illustrated in Fig. 19. Ultimate compression strength (UCSs – direct compression method) average 2800 MPa is independent on strain rate in the range of $1\div100$ s^{-1} but the strain clearly decreases from 0.75 to 0.20 in the strain rate increasing under direct compression. In the same strain rate range UCS (indirect compression method) decreases from about 2700 to 2500 MPa and strain decreases from 0.65 to 0.28. It was found that at the higher strain rate, the higher difference in compression stress were obtained between the samples deformed directly and indirectly. The maximum difference of stress of approximately 400 MPa was found for the B-210 nanostructured bainitic steel at strain rate of 100 s^{-1}. Commercial martensitic armour steel of UTS 2250 MPa is characterised by UCS about 2700 MPa at strain about 0.50 determined in quasi-static compression [26].

The results clearly indicate that retained austenite is more prone to deformation (transformation in martensite) under dynamic direct compression. Lower strain during direct compression indicates that martensite with higher carbon content than average content in the steel, formed during deformation, as a result of deformation-induced transformation of retained austenite. Martensite induces higher stress but lower strain until specimen failure during uniaxial direct compression. It is suggested that mechanical stability of retained austenite is lower in the direct compression in comparison with indirect compression.

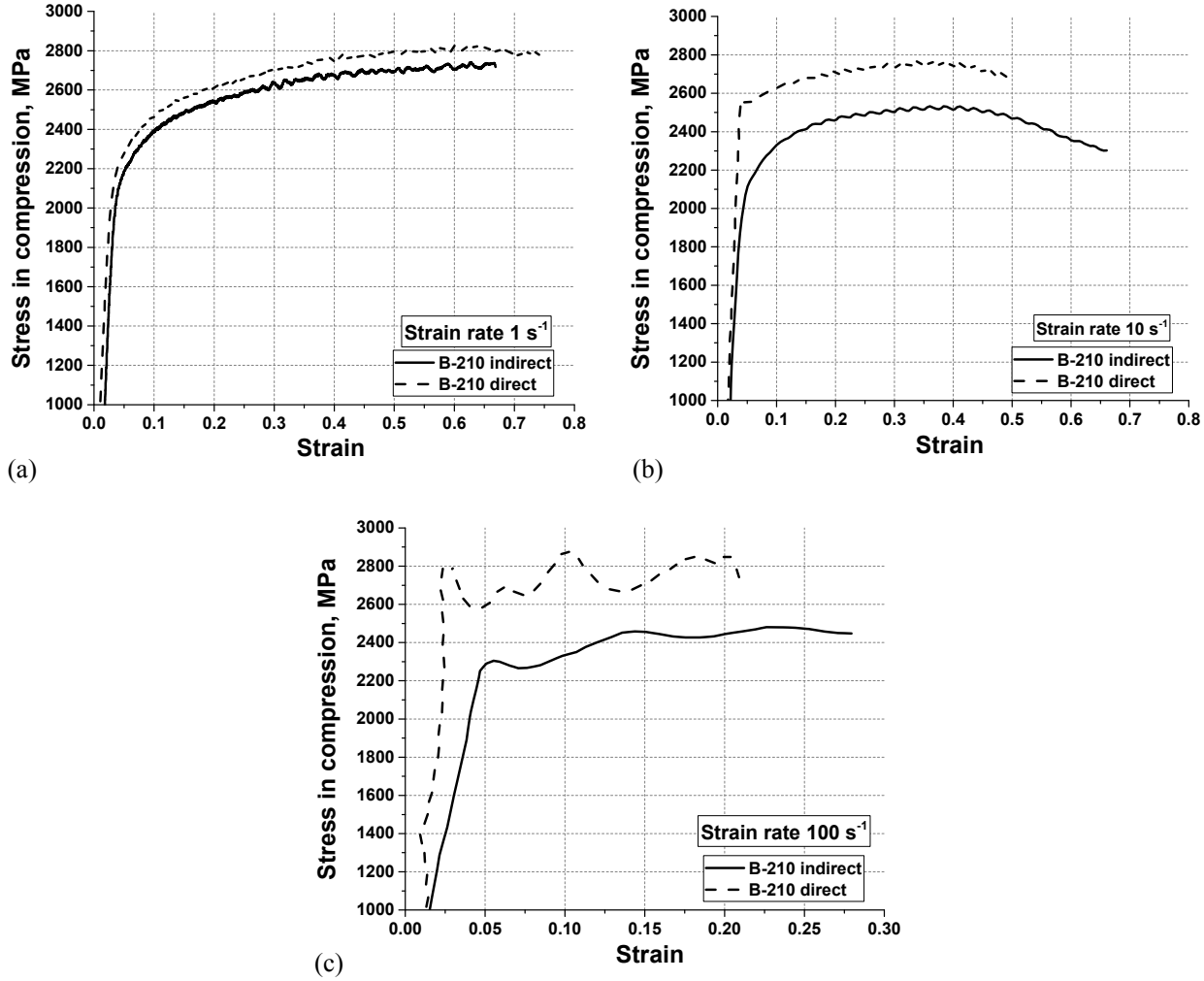

Fig. 19. Compression curves of the B-210 nanostructured bainitic steel obtained under direct and indirect compression with a strain rate of (a) 1 s^{-1}; (b) 10 s^{-1} and (c) 100 s^{-1}

4.5. Macrostructure examination and hardness measurements results after uniaxial direct compression

An example of macrostructure as well as the results of hardness measurements for the B-210 variant of nanostructured bainitic steel after direct compression test is presented in Fig. 20. No ASBs and cracks were found in the specimen with hardness of up to 800 HV detected within the area of stress and strain localisation (Fig. 20b). First adiabatic shear bands with a hardness of 865 HV were observed in the specimen of variant B-210 which cracked during direct compression. The hardness level of 790÷800 HV correspond to microstructure consists only

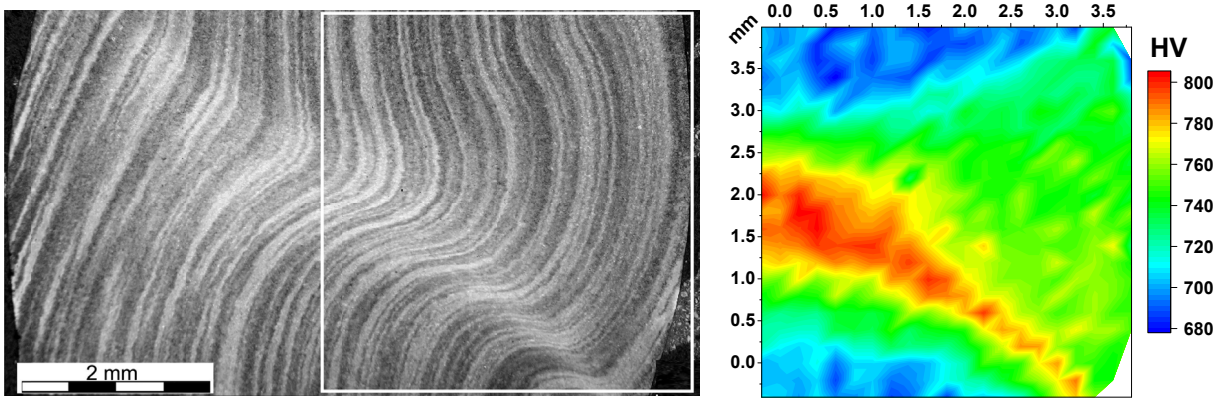

Fig. 20. Macrostructure (a) and hardness distribution (b) within the area of strain localisation formed during uniaxial direct compression. Nanostructured bainitic steel – variant B-210; strain rate 10 s^{-1}; strain 0.5. White square indicates the area of hardness measurements (b)

of martensite of average carbon content in this steel grade. The average hardness of undeformed matrix of the B-210 variant is 620 HV, so local increasing of the hardness results from transformation of retained carbon enriched austenite to martensite.

5. Summary

Investigation of nanostructured bainitic steel under dynamic shear and direct and indirect uniaxial compression were carried out to indicate the material's properties important for high ability to absorb and dissipate impact energy. Variant of nanostructured bainitic steel of isothermal transformation temperature 210°C was used in the investigation. It was assumed that shear strength, shear energy and toughness under shearing and direct compressive strength are the crucial properties for steel grades applied at dynamic conditions.

The shear strength and shear energy of nanostructured bainitic steel were determined. The B-210 nanostructured bainitic steel is characterised by dynamic shear strength in the range of 1400÷1550 MPa at the punch velocity of up to 10 m/s. Total shear energy clearly decreases from about 14 to 7×10^9 J/m^3 when punch velocity (strain rate) increases up to 10 m/s.

Adiabatic shear bands (ASBs) formed in strain localisation zones produced in shear tests. Susceptibility of nanostructured bainitic steel to ASB formation was assessed. Two main factors: strain rate and value of strain – were indicated as significant for the process of ASBs formation. Moreover, the formation of ASBs is influenced by the method of deformation that causes shear stress and strain concentration zones. Adiabatic shear bands formed in the examined variant of nanostructured bainitic steel with the average hardness of 620 HV, when the local hardness of matrix exceeded approximately 800 HV. Hardness of the bands within the range of 850÷1150 HV was determined for deformed material.

It was found that compression with direct loading induces higher stress level in the range of 85÷400 MPa depending on strain rate as compared to indirect compression. Strain to failure in compression tests decreases with the increase in strain rate. Under direct compression strain within the range of 0.75÷0.20 was obtained at the strain rate respectively of 1 and 100 s^{-1} for variant B-210 of nanostructured bainitic steel. First adiabatic shear bands at direct compression tests formed in the shearing zones of hardness exceeding 800 HV.

6. Conclusions

From the results presented in the previous sections, the following conclusions can be made:

1. Dynamic shear strength decreases from 1500 to 1400 MPa with punch velocity increases in the range of up to 800 mm/s. Dynamic shear strength of 1460 MPa at punch velocity of about 10 m/s was determined at Hopkinson bar experiments.
2. Energy of shearing decreases from 14 to 6 x10^9 J/m^3 with punch velocity (strain rate) increases in the range of up to 800 mm/s. Shear energy of 7×10^9 J/m^3 was determined at the punch velocity of about 10 m/s in Hopkinson bar tests.
3. Adiabatic shear bands occur when the hardness exceeds of 800 HV at the average hardness of the steel of about 620 HV. Two regions of different morphologies were found in the ASBs correspond to deformed and transformed in the core of the band.
4. ASBs are crucial microstructure elements influence ductility and susceptibility to cracking during dynamic deformation because of crack nucleation and propagation in this areas and in the transition zone between bands and matrix of the steel.
5. It was found that deformation induced transformation of retained austenite to martensite occurs in the dynamic shear zone. The volume fraction of retained austenite decreases from 20% to about 10% in the shearing zone with ASBs formation.

Acknowledgements

This work was financially supported by The National Centre for Research and Development (POIR-04.01.04-00-0047/16, Project "Development of production technology of light observation-protective container (LOOK) made of nanostructured ultrastrength steels").

REFERENCES

[1] F.G. Caballero, H.K.D.H. Bhadeshia, K.J.A. Mawella, D.G. Jones, P. Brown, Mater. Sci. Technol. **18**, 279-284 (2002).
[2] C. Garcia-Mateo, F.G. Caballero, H.K.D.H. Bhadeshia, ISIJ Int. **43**, 1238-1243 (2003).
[3] C. Garcia-Mateo, F.G. Caballero, H.K.D.H. Bhadeshia, ISIJ Int. **43**, 1821-1825 (2003).
[4] F.G. Caballero, H.K.D.H. Bhadeshia, Curr. Opin. Solid State Mater. Sci. **8**, 251-257 (2004).
[5] B. Garbarz, W. Burian, Steel Res. Int. **85** (12), 1620-1628 (2014).
[6] B. Garbarz, B. Niżnik-Harańczyk, Mater. Sci. Technol. **31** (7), 773-780 (2015).
[7] W. Liu, J. Qu, H. Shao, J. Mater. Proc. Technol. **69**, 186-189 (1997).
[8] C. Garcia-Mateo, F.G. Caballero, Mat. Trans. **46** (8), 1839-1846 (2005).
[9] L. Morales-Rivas, C. Garcia-Mateo, M. Kuntz, T. Sourmail, F.G. Caballero, Mat. Sci. and Eng. **A662**, 169-177 (2016).
[10] E. Kozeschnik, H.K.D.H. Bhadeshia, Mat. Sci. and Technol. **24**, 343-347 (2008).
[11] T. Sourmail, C. Garcia-Mateo, F.G. Caballero, L. Morales-Rivas, R. Rementeria, M. Kuntz, Metals **7** (1), 31-38 (2017).
[12] L. Morales-Rivas, C. Garcia-Mateo, T. Sourmail, M. Kuntz, R. Rementeria, F.G. Caballero, Metals **6** (12), 302-322 (2016).
[13] W. Burian, J. Marcisz, B. Garbarz, L. Starczewski, Arch. of Metall. and Mater. **59**, (3), 1211-1216 (2014).

[14] J. Marcisz, W. Burian, J. Stępień , L. Starczewski, M. Wnuk, J. Janiszewski, 28th International Symposium on Ballistics, Atlanta, USA, 1348-1361 (2014).

[15] B. Garbarz, J. Marcisz, W. Burian, A. Wiśniewski, Problemy Techniki Uzbrojenia. Biuletyn Naukowy Wojskowego Instytutu Technicznego Uzbrojenia **118** (2), 41-49 (2011) (in polish).

[16] J. Marcisz, B. Garbarz, W. Burian, A. Wiśniewski, 26th International Symposium on Ballistics, Miami, USA, 1595-1606 (2011).

[17] L.C.D. Fielding, H.K.D.H. Bhadeshia, Mat. Sci. and Technol. **30**, 812-817 (2014).

[18] T.W. Wright, The physics and mathematics of adiabatic shear bands, Cambridge University Press, 2002

[19] S.M. Walley, Metall. and Mater. Trans. A **38A**, 2629-2654 (2007).

[20] M.A. Meyers, V.F. Nesterenko, J.C. LaSalvia, Qing Xue, Mater. Sci. and Eng. **A317**, 204-225 (2001).

[21] B. Avishan, A. Sefidgar, S. Yazdani, J. of Mater. Sci. **54** (4), 3455-3468 (2019).

[22] Y.T. Tsai, C.R. Lin, W.S. Lee, C.Y. Huang, J.R. Yang, Scripta Materialia **115**, 46-51 (2016).

[23] Y.-T. Tsai, Y.-W. Chen, J.-R. Yang, Procedia Engineering **207**, 1862-1867 (2017).

[24] D.-T. Chung, S.-K. Moon, Y.-H. Yoo, Journal de Physique IV, Colloque C8, supplement au Journal de Physique III **4**, 547-552, (1994).

[25] L.C.D. Fielding, H.K.D.H. Bhadeshia, Mat. Sci. and Technol. **30**, 812-817 (2014).

[26] H. Nahme, E. Lach, Journal de Physique IV **7**, 373-378 (1997).